ELSEVIER

Ceramics International 28 (2002) 881–886

CERAMICS INTERNATIONAL

www.elsevier.com/locate/ceramint

Properties and microstructure of sintered incinerator bottom ash

S. Bethanis, C.R. Cheeseman*, C.J. Sollars

Centre for Environmental Control and Waste Management, Department of Civil and Environmental Engineering, Imperial College of Science, Technology and Medicine, London SW7 2BU, UK

Received 11 November 2001; received in revised form 25 February 2002; accepted 18 March 2002

Abstract

The fraction of incinerator bottom ash with a particle size less than 8 mm produced at a commercial municipal solid waste incinerator was wet milled, dried, compacted and sintered at a range of temperatures to form ceramic materials. The effects of milled ash particle size distribution, powder compaction pressure and sintering temperature were investigated, and the materials formed characterised by X-ray diffraction (XRD), scanning electron microscopy (SEM) and thermal analysis (TG/DTA). The main minerals present in the milled ash were quartz (SiO_2) and calcite ($CaCO_3$). Sintered densities of materials produced from ash milled to 95% less than 27 μm increased from 1.38 to 2.63 g/cm^3 on increasing the sintering temperature from 1020 to 1080 °C. Firing above 1080 °C caused a rapid decrease in density and sample expansion. The principal crystalline phase present in the high-density material was diopside ($CaMgSi_2O_6$). This work shows that a significant fraction of incinerator bottom ash can be processed to form sintered materials with properties controlled by ash particle size distribution and sintering conditions.

Keywords: A. Sintering; Incinerator bottom ash; Waste reuse; Ceramic processing; Diopside; Waste management

1. Introduction

Although landfill remains the dominant disposal method for municipal solid waste (MSW), many industrialised countries are increasingly considering waste incineration to be a viable alternative. This is because in many parts of the world readily available landfill void space is becoming exhausted and there are often significant problems associated with locating new landfill sites. The potential long-term adverse environmental effects and costs of landfilling are now widely recognised. Incineration has the advantage that the plant can be located close to where waste is generated and can use the significant energy content of MSW to produce electricity and/or hot water for distribution to the local community. This can be efficiently achieved in modern "energy from waste" (EfW) plants that are designed to have minimal environmental impact [1]. Disposal of MSW incinerator ashes to landfill occupies only one-tenth the volume of the original waste, conserving void space. However, avoiding landfill disposal of incinerator ash by developing reuse applications is clearly the preferred option and has been the subject of extensive research [2–4].

Incinerator bottom ash (IBA) is a highly heterogeneous burnt-out mixture of slag, ferrous and non-ferrous metal, ceramics, glass, other non-combustibles and residual organic matter [5–7]. The extreme heterogeneity of bottom ash combined with the potential leachability of heavy metals means that some form of processing is likely to be required to improve the characteristics of the ash prior to utilisation in most civil engineering applications. The development of "value added" reuse products would have particular benefits both in terms of resource recovery and protection of the environment.

High temperature sintering can convert particulate inorganic waste materials into more environmentally benign products that have no adverse effect on the environment and public health. A number of researchers have demonstrated reduced leaching from sintered products compared to the original waste [8–10]. The use of waste incinerator fly ash, filter dusts and bottom ash

* Corresponding author. Tel.: +44-207-594-5971; fax: +44-207-823-9401.

E-mail address: c.cheeseman@ic.ac.uk (C.R. Cheeseman).

0272-8842/02/$22.00
PII: S0272-8842(02)00068-8

to produce glasses and glass-ceramics has been reported [11–14]. This has generally involved heating the wastes to high temperatures (>1300 °C) to cause vitrification prior to subsequent heat treatment to induce controlled crystallisation.

The aim of this work was to investigate the properties of materials produced by conventional powder processing and liquid phase sintering of MSW incinerator bottom ash at relatively low temperatures. The effects of particle size distribution, compaction pressure and firing temperature on the physical properties, mineralogy and microstructure of uniaxially pressed and sintered samples have been studied.

2. Experiments

2.1. Material and processing

MSW bottom ash produced at the South-East London Combined Heat and Power (SELCHP) EfW plant was used for this research. This is one of the largest plants currently operating in the UK, with a capacity to burn 420,000 tonnes per year of household waste. It uses well-established mass-burn incineration technology and generates 34 MW of electricity.

The bottom ash sample used in these experiments had been weathered for between 6–8 weeks and the majority of the ferrous and non-ferrous metals removed by magnetic separation. The remaining ash was sieved to separate different size fractions and ash with a particle size less than 8 mm collected. This represents approximately 45% by mass of the total weathered ash and is the fraction for which alternative reuse applications have not so far been commercially developed. The material had considerably improved homogeneity compared to the as-produced ash.

Ball milling was used to reduce and control the particle size distribution of bottom ash samples. This processing technique is widely used in the ceramics industry and has the advantage that in addition to reducing particle size it also produces a more homogenous slurry suitable for subsequent processing. Ash samples were processed using a 3 litre polypropylene mill containing high-density alumina milling media, rotating at approximately 50 rpm. Batches of 500 g of ash were wet milled for 2, 8 and 16 h using a water to solids ratio of 2. The particle size distributions of the milled slurries in the range 0.4–900 μm were determined using laser diffraction (Beckman Coulter, LS-100).

Milled slurries were passed through a 355 μm sieve and de-watered by pressure filtration through a Whatman GF/C filter paper using a stainless steel extraction vessel. The filter cakes formed were oven-dried overnight at 105 °C and ground in a pestle and mortar to produce a fine, consistent grey powder.

2.2. Milled ash characterisation

The chemical compositions of milled powders were determined by lithium metaborate fusion, with digests analyzed using inductively coupled plasma atomic emission spectroscopy (ICP-AES). The loss on ignition (L.O.I) was obtained by heating dried milled ash to 1000 °C.

Crystalline phases present in milled powders were analysed by X-ray diffraction (XRD) (Phillips PW1830) using 50 mA and 40 kV, CuK_α radiation.

The thermal stability of the milled ash was characterised from 25 to 1200 °C using a Stanton Redcroft thermal analyser (STA-1500 Series) at a heating rate of 6 °C/min in air, using calcined alumina as reference material. Weight and energy changes in 15 mg samples were recorded as thermogravimetric (TG) and differential thermal analysis (DTA) data.

2.3. Production of sintered samples

The milled dried bottom ash powder was uniaxially pressed at 32 MPa using a stainless steel die, to form 2 cm diameter and approximately 2.2 cm high cylindrical "green" samples. These were sintered at temperatures between 1020 and 1100 °C, using a ramp rate of 6 °C/min and a dwell time of 1 h. In addition, the effect of compaction pressure on the physical properties of the "green" and sintered samples was investigated by pressing 16 h-milled ash powder at 4, 8, 16, 32 and 64 MPa prior to sintering at 1080 °C for 1 h.

2.4. Characterisation of sintered samples

Dry density, shrinkage and water absorption was determined for sintered samples. Density was calculated using Archimedes' method and water absorption capacity determined from the increase in weight of "surface dry" samples after being submerged for 24 h. The percentage shrinkage of the sintered samples was determined from the reduction in sample diameter.

Sintered samples were ground to <150 μm for XRD to determine the crystalline phases present and gold-coated fracture surfaces of sintered samples were examined using scanning electron microscopy (SEM-Phillips XL40).

3. Results and discussion

3.1. Particle size distribution

The effect of milling on the particle size distribution of bottom ash is shown in Fig. 1 for 2, 8 and 16 h-milled ash compared to as-received ash. Fifty percent of the volume (d_{50} value) of the as-received ash was 295 μm,

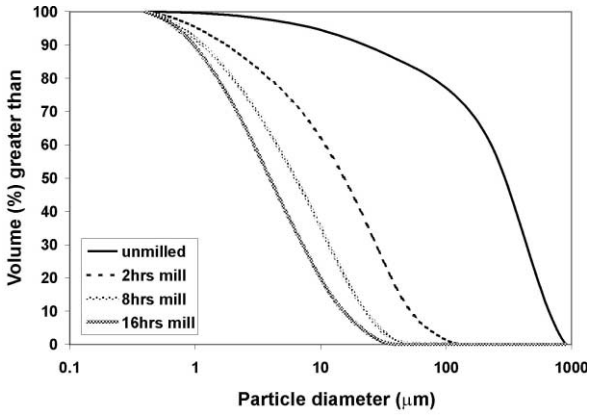

Fig. 1. Particle size distribution of as-received and milled bottom ash.

and this decreased to 15 μm after 2 h milling. Corresponding d_{50} values for 8 and 16 h-milled ash were 6.2 and 3.9 μm, with d_{95} values of 0.8 and 0.7 μm respectively.

3.2. Chemical composition of milled ash

Averaged data from chemical analysis of 6 samples of milled bottom ash is summarised in Table 1. Approximately 75–85% w/w of the milled bottom ash consists of silica (SiO_2), alumina (Al_2O_3), iron (Fe_2O_3) and calcium oxides (CaO). Sodium, potassium, magnesium, phosphate and titanium were also present. Heavy metals of environmental concern at high concentrations included Zn (>2000 mg/kg), Ni (80–120 mg/kg), Cu (650–800 mg/kg) and Cr (300–350 mg/kg). The loss on ignition of dried milled ash ranged from 11.8 to 12.3% w/w indicating that a significant fraction of unburnt organic carbon remained in the ash.

3.3. Thermal behaviour of milled powder

TG/DTA data of milled ash is shown in Fig. 2. Initial weight loss from ambient to 120 °C was due to evaporation of remaining moisture. Studies on other organic containing wastes have reported weight losses up to 550 °C resulting from the release of occluded gases, primarily CO_2 [15]. A significant weight loss accounting for 6.1% of original sample weight occurs between 600 and 750 °C and is associated with an endothermic peak at 728 °C. Samples heated to 650 and 750 °C for 1 h were analysed by XRD and this confirmed decomposition of calcite ($CaCO_3$) to lime (CaO) with consequent loss of CO_2 [16]. A further weight loss of 1.4% between approximately 1050 and 1140 °C is thought to be due to evolution of gaseous SO_2 from decomposition of alkali metal sulphates [17,18].

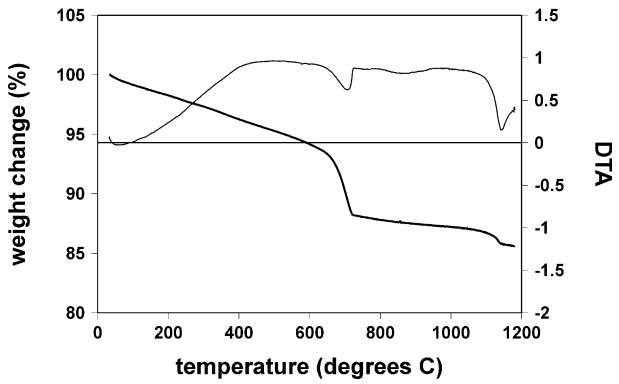

Fig. 2. TG/DTA curve for milled ash.

Table 1
Chemical composition of milled ash

Component	Wt.%	Element	Range (mg/kg)
SiO_2	40.09–42.12	Ba	1000–1050
Al_2O_3	9.92–14.20	Be	1.4
Fe_2O_3	6.20–6.60	Co	<15–20
CaO	18.42–20.01	Cr	300–350
MgO	1.79–1.90	Cu	650–800
Na_2O	2.60–2.75	Ni	80–120
K_2O	0.86–0.92	Sr	280–310
P_2O_5	1.34–1.44	Zn	>2000
TiO_2	1.00–1.14	Zr	115–200
MnO	0.08		
L.O.I.	11.80–12.30		

3.4. Physical properties of sintered samples

The effect of temperature on the density and shrinkage of sintered milled incinerator bottom ash samples is shown in Figs. 3 and 4. The particle size controls these properties, with more extensively milled ash samples having higher sintered densities and higher shrinkage. Increasing the sintering temperature to 1080 °C increases densification for 8 and 16-h milled samples and maximum densities of 2.6 g/cm^3 were achieved with 20% shrinkage. Firing above 1080 °C resulted in a rapid decrease in density and sample expansion. The coarser

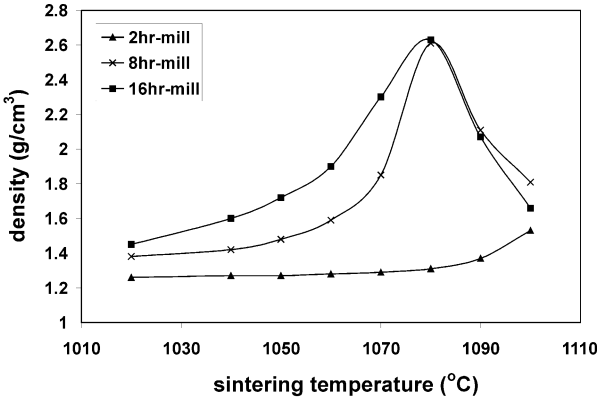

Fig. 3. Effect of sintering temperature (1h dwell) on the density of IBA samples pressed at 32 MPa.

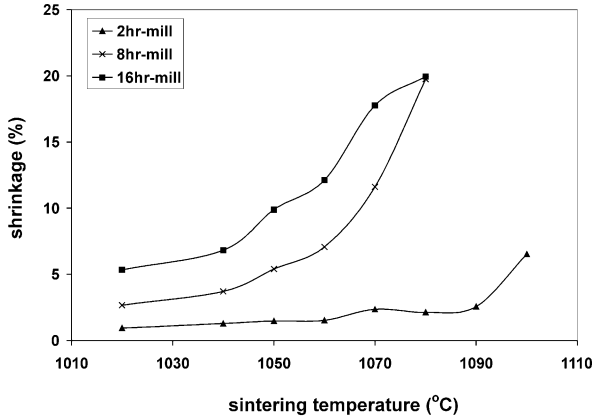

Fig. 4. Effect of sintering temperature (1h dwell) on the shrinkage of IBA samples pressed at 32 MPa.

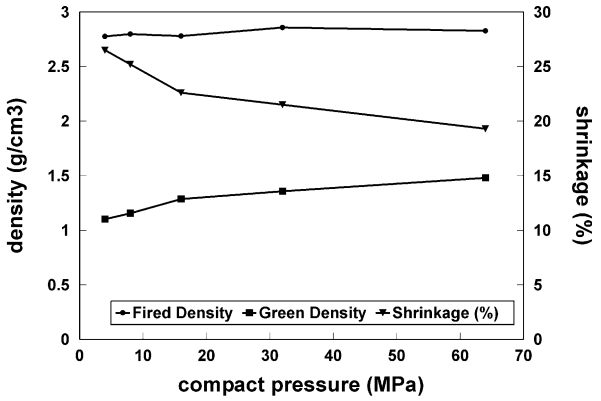

Fig. 6. Effect of compact pressure on the "green" density, fired density and shrinkage of 16 h-milled IBA sintered at 1080 °C.

particle size distribution of the 2 h-milled samples produced much lower sintered densities (1.3 g/cm^3) and increase in density with sintering temperature was greatly reduced.

Fig. 5 shows the effect of sintering temperature on water absorption. This decreases with increasing temperature due to a reduction in the open, water accessible porosity. The 8 and 16 h-milled samples become practically impermeable when sintered above 1080 °C, while the 2 hour-milled samples show high water absorption (30–45%) at all temperatures, associated with a lower density, highly porous microstructure.

The effect of compaction pressure on "green" and fired densities and shrinkage of 16 hour-milled ash samples sintered at 1080 °C for 1 h is shown in Fig. 6. Increasing the compaction pressure had minimal effect on fired densities, but shrinkage was dependent on "green" density and, therefore, the compaction pressure. Samples compacted at higher pressures had increased "green" densities and exhibited less shrinkage than samples compacted at low pressures.

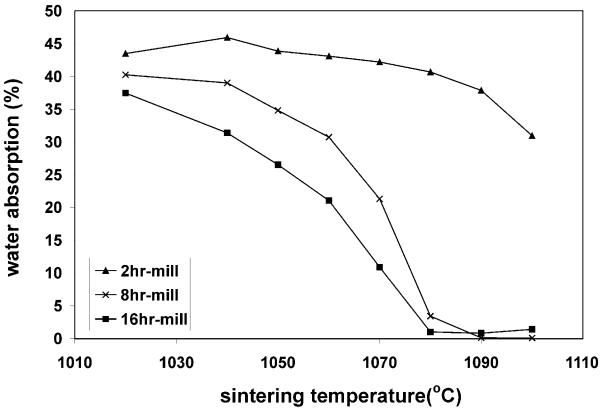

Fig. 5. Effect of sintering temperature (1h dwell) on the water absorption of IBA samples pressed at 32 MPa.

3.5. Mineralogy of milled and sintered ash

X-ray diffractograms of the 16 h-milled and sintered ash at 1080 °C are shown in Fig. 7 and the data is summarised in Table 2. The major crystalline phases identified in the milled ash were quartz (SiO_2) and calcite ($CaCO_3$), ghelenite ($Ca_2Al_2SiO_7$) and hematite (Fe_2O_3) and these minerals have previously been identified as major components present in incinerator bottom ashes [6,16,19,20] and coal fly ashes [21]. Analysis of the milled ash sintered at the maximum density temperature revealed that diopside ($CaMgSi_2O_6$) was the principal

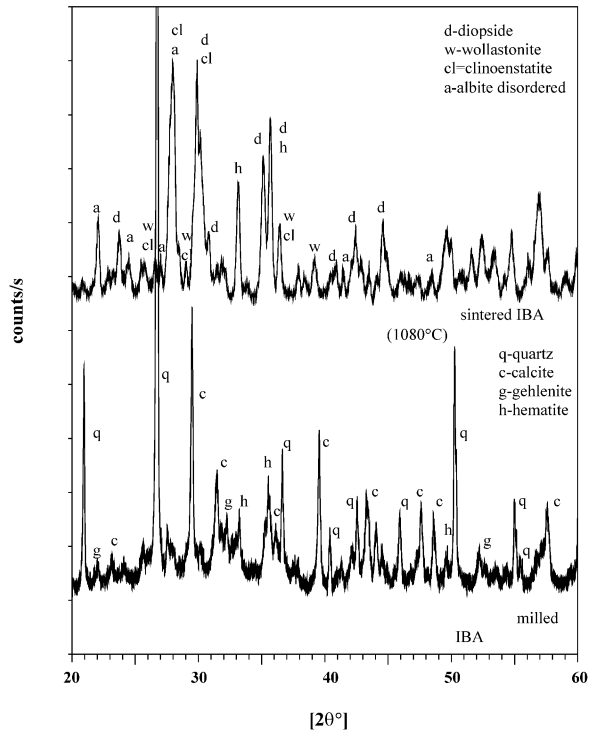

Fig. 7. X-ray diffractograms of milled and sintered IBA at 1080 °C.

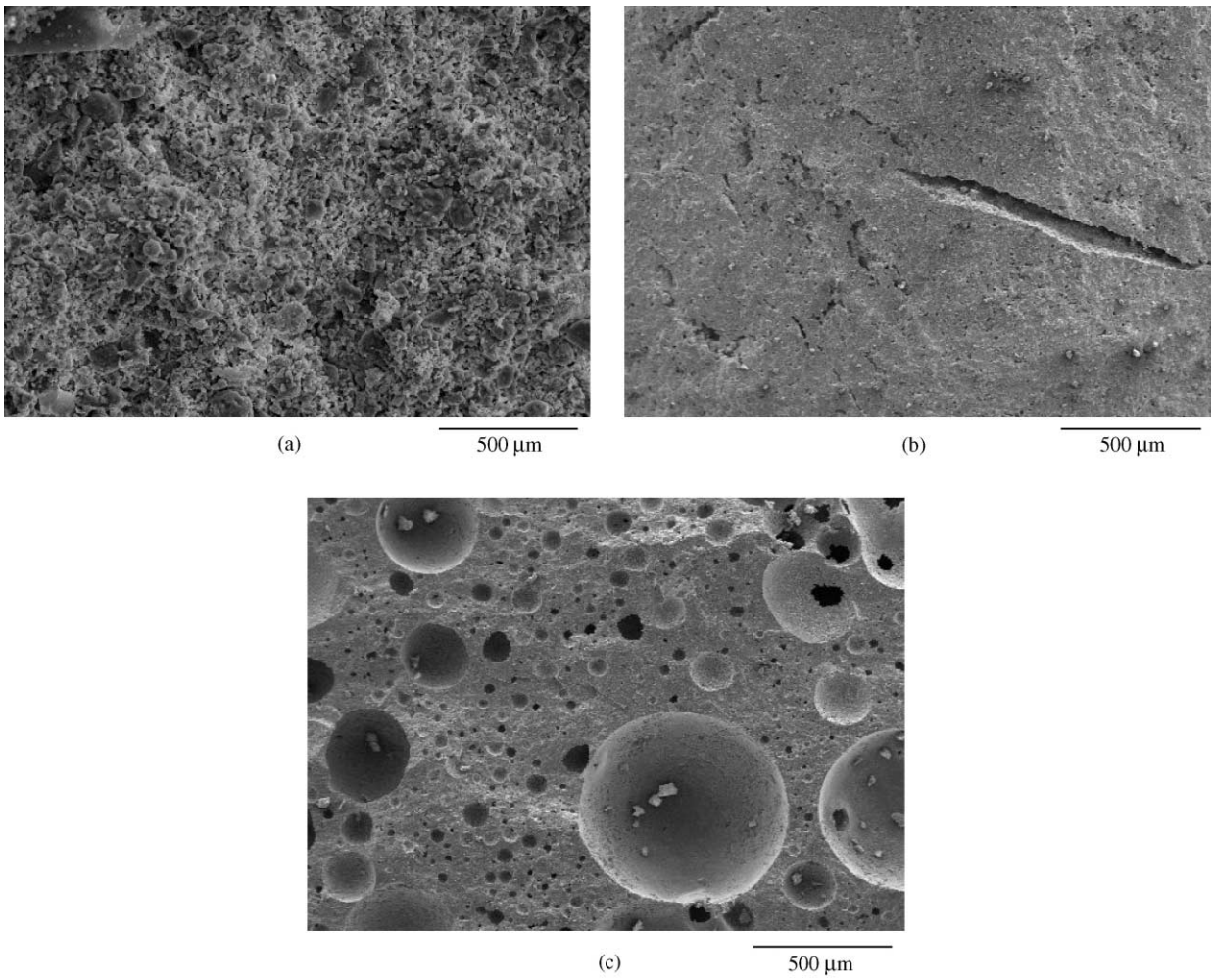

Fig. 8. SEM micrograph of 16 h-milled IBA sintered at (a) 1020; (b) 1080; (c) 1100 °C.

crystalline phase, with significant amounts of clinoenstatite ($MgSiO_3$) and wollastonite ($CaSiO_3$), and minor amounts of albite ($NaAlSi_3O_8$) and hematite. The quartz and calcite peaks decreased on sintering and had completely disappeared by 1080 °C, due to the formation of crystals of the pyroxenoids group, such as diopside and wollastonite. Diopside is an important rock forming mineral in several metamorphic and basic to ultra-basic igneous rocks. It is reported to form the major crystalline phase in glass-ceramics formed from vitrified municipal incinerator fly ash, filter dusts and industrial waste [11,14,22].

Table 2
Mineralogy of milled and sintered IBA

Mineral	Milled[a]	Sintered (1080 °C)
Quartz: SiO_2	+ + + +	
Calcite: $CaCO_3$	+ + +	
Ghelenite: $Ca_2Al_2SiO_7$	+ +	
Hematite: Fe_2O_3	+ +	+
Diopside: $CaMgSi_2O_6$		+ + + +
Clinoenstatite: $MgSiO_3$		+ + +
Wollastonite: $CaSiO_3$		+ + +
Albite: $NaAlSi_3O_8$		+ +

[a] + + + +, Very strong; + + +, strong; + +, weak; +, possible.

3.6. Microstructural analysis of sintered samples

SEM micrographs of fracture surfaces of 16 h-milled incinerator ash samples sintered at 1020, 1080 and 1100 °C are shown in Figs. 8(a)–(c). Samples fired at 1020 °C appeared to be poorly sintered with a granular fracture surface due to high porosity. The fracture surfaces of the samples sintered at 1080 °C showed a dense, well-sintered microstructure, although occasional elongated cavities were clearly evident. The fracture surfaces of the samples sintered at 1100 °C were very different with reduced densities and sample expansion clearly associated with the formation of large isolated, approximately spherical closed pores. The development of this foamed internal structure is believed to be due to evolution of SO_2 from decomposition of alkaline metal sulphates, together with melting of a significant amount of the glassy material present in the ash [17,18].

4. Conclusions

1. The fine fraction (< 8 mm) of MSW incinerator bottom ash can be processed and sintered to form new materials using conventional ceramic processing technology involving ball milling, drying, powder compaction and sintering.
2. The particle size distribution of milled MSW incinerator bottom ash and sintering temperature control fired density, shrinkage, water absorption and microstructural characteristics.
3. Samples prepared from ash milled to a $d_{95} <$ 27 μm increased in density with sintering temperature up to 1080 °C. The maximum density obtained was 2.6 g/cm^3.
4. Firing above 1080 °C resulted in a density decrease and sample expansion, associated with the formation of an extensive spherical porosity, possibly due to SO_4 evolution in the presence of a low viscosity glassy phase.
5. Quartz and calcite were the major crystalline phases present in the milled MSW incinerator bottom ash. Diopside ($CaMgSi_2O_6$) was formed during sintering and was the major crystalline phase present in high-density sintered MSW incinerator bottom ash.

Acknowledgements

This research was funded by the UK Engineering and Physical Sciences Research Council (EPSRC) under the Waste Minimisation through Recycling, Reuse and Recovery in Industry programme (project GR/M 51444).

References

[1] P.T. Williams, Waste Treatment and Disposal, John Wiley and Sons, Chichester, UK, 1998.
[2] N.-B. Chang, H.P. Wang, W.L. Huang, K.S. Lin, The assessment of reuse potential for municipal solid waste and refuse-derived fuel incineration ashes, Resources Conservation and Recycling 25 (1999) 255–270.
[3] J. Pera, L. Coutaz, J. Ambroise, M. Chababbet, Use of incinerator bottom ash in concrete, Cement and Concrete Research 27 (1) (1997) 1–5.
[4] E.R. Berg, J.A. Neal, Municipal solid waste bottom ash as Portland cement concrete ingredient, Journal of Materials in Civil Engineering 10 (1998) 168–173.
[5] J.M. Chimenos, M. Segarra, M.A. Fernández, F. Espiell, Characterisation of the bottom ash in municipal solid waste incinerator, Journal of Hazardous Materials 64 (1999) 211–222.
[6] G. Pfrang-Stotz, J. Reichelt, R. Roos, Chemical-mineralogical valuation of the leachate potential of municipal solid waste incineration (MSWI) bottom ashes, in: G.R. Woolley, J.J.J.M. Goumans, J.P. Wainwright (Eds.), Waste Materials in Construction, Elsevier, Amsterdam, 2000, pp. 975–983.
[7] C.C. Wiles, Municipal solid waste combustion ash: State-of-the-knowledge, Journal of Hazardous Materials 47 (1996) 325–344.
[8] K.-S. Wang, K.-Y. Chiang, J.-K. Perng, C.-J. Sun, The characteristics study on sintering of municipal solid waste incinerator ashes, Journal of Hazardous Materials 59 (1998) 201–210.
[9] M.A. Sørensen, E.P.B. Mogensen, K. Lundtorp, D.L. Jensen, T.H. Christensen, High temperature co-treatment of bottom ash and stabilised fly ashes from waste incineration, Waste Management 21 (2001) 555–562.
[10] A. Selinger, V. Schmidt, Investigation of sintering processes in bottom ash to promote the reuse in civil construction, Parts 1 & 2, in: G.R. Woolley, J.J.J.M. Goumans, P.J. Wainwright (Eds.), Waste Materials in Construction: Putting Theory into Practice, Elsevier, Amsterdam, 1997, pp. 41–58.
[11] A.R. Boccaccini, M. Petitmermet, E. Wintermantel, Glass-ceramics from municipal incinerator fly ash, Ceramic Bulletin 76 (11) (1997) 75–78.
[12] M. Romero, J.Ma Rincón, R.D. Rawlings, A.R. Boccaccini, Use of vitrified urban incinerator waste as raw material for production of sintered glass-ceramics, Materials Research Bulletin 36 (2001) 383–395.
[13] L. Barbieri, A. Corradi, I. Lancellotti, Bulk and sintered glass-ceramics by recycling municipal incinerator bottom ash, Journal of the European Ceramic Society 20 (10) (2000) 637–1643.
[14] A.R. Boccaccini, M. Kopf, W. Stumpfe, Glass-ceramics from filter dusts from waste incinerators, Ceramics International 21 (1995) 231–235.
[15] G. Zheng, J.A. Kozinski, Thermal events during the combustion of biomass residue, Fuel 79 (2000) 181–192.
[16] T. Mangialardi, L. Piga, G. Schena, P. Sirini, Characteristics of MSW incinerator ash for use in concrete, Environmental Engineering Science 15 (4) (1998) 291–297.
[17] V.M. Slavo, R. Campostrini, S. Maurina, G. Carturan, M. Mongheddu, G. Budroni, G. Cocco, Bauxite 'red mud' in the ceramic industry, Part 1: thermal behaviour, Journal of the European Ceramic Society 20 (2000) 235–244.
[18] K.H. Stern, E.L. Weise, High Temperature Properties and Decomposition of Inorganic Salts, Part 1: Sulphates, NSRDS-National Bureau of Standards 7, USA, 1966.
[19] C. Zevenbergen, T. Vander Wood, J.P. Bradley, Morphological and chemical properties of MSWI bottom ash with respect to the glassy constituents, Hazardous Waste and Hazardous Materials 11 (3) (1994) 371–383.
[20] C.S. Kirby, J.D. Rimstidt, Mineralogy and surface properties of municipal solid waste ash, Environmental Science and Technology 27 (1993) 652–660.
[21] V. Sakorafa, F. Burragato, K. Michailidis, Mineralogy, geochemistry and physical properties of fly ash from the Megalopolis lignite fields, Peloponnese, Southern Greece, Fuel 75 (1996) 419–423.
[22] L. Barbieri, A.C. Bonamartini, I. Lancellotti, Alkaline and alkaline-earth silicate glasses and glass-ceramics from municipal and industrial wastes, Journal of the European Ceramic Society 20 (2000) 2477–2483.